



# COMPARATIVE STUDY ON STRUCTURAL, MORPHOLOGICAL AND OPTICAL PROPERTIES OF TRANSITION METAL (MN AND AG) DOPED AND UN-DOPED ZINC OXIDE NANOPARTICLES

Pavithra Dhanasekaran<sup>1</sup>, Roopakala Kottayi<sup>1\*</sup>, Ilangovan Veerappan<sup>1</sup>

<sup>1</sup> Department of Physics, Kanchi Mamunivar center for Postgraduate Studies,

## ABSTRACT

Nowadays, metal oxide semiconductor nanoparticles (NPs) have great attention due to their excellent material properties such as broad bandgap, high electron mobility, etc. Doping of these metal oxides with transition metals improves their electrochemical and optical properties. Herein, pure zinc oxide (ZnO) NPs, Ag-doped zinc oxide (Ag-ZnO) NPs and Mn-doped zinc oxide (Mn-ZnO) NPs were synthesized by sol-gel method. The structure and morphology of the synthesized NPs were examined by X-ray diffraction spectra, transmission electron microscope images, energy dispersive X-ray diffraction spectra, and scanning electron microscope images analysis. It observed that all three NPs have hexagonal wurtzite structures. Compared to pure ZnO NPs, the doped NPs show more agglomeration. The size of the NPs was calculated to be 16 nm, 22 nm and 36 nm respectively for ZnO, Mn-ZnO and Ag-ZnO, respectively. Structural analysis and morphological analysis reveal that doping of Mn and Ag didn't affect the crystalline structure of ZnO NPs but surface area varies due to the lattice defect. Uv-vis absorption spectra reveal the broad light absorption capability of the Ag-doped ZnO NPs. Photoluminance emission intensity was decreased in the following order: ZnO > Mn-ZnO > Ag-ZnO. Quenching in the emission intensity reveals the enhanced charge transfer rate. From the Tauc plot analysis, band gap energy was estimated. Hence, optical analysis exposes the Ag-doped ZnO has superior absorption and emission property.

### Highlights

- Hexagonal wurtzite structured, ZnO NPs, Mn-ZnO NPs and Ag-ZnO NPs synthesized by a Sol-Gel method.
- Structural, morphological and optical properties of the synthesised NPs were studied and compared.
- The structural analysis and morphological analysis reveal that doping of Mn and Ag didn't affect the crystalline structure of ZnO NPs but surface area varies due to the lattice defect.
- The optical analysis expose the Ag-doped ZnO has superior absorption and emission property.

**KEYWORDS:** Metal Oxides, Doping, Tauc Plot, Bandgap, Sol- Gel method.

## 1. INTRODUCTION

One of the great potentials that the metal oxides NPs hold in various applications owing to their significant capacity to absorb a variety of molecules. Among the other metal oxides, zinc oxide (ZnO) NPs have recognized itself as interesting materials because of its unique physical and chemical properties. Mainly, ZnO is a semiconductor in group II-VI, with band gap energy of 3.37 eV. ZnO NPs can occur in different structures. However, undoped ZnO (pure ZnO) NPs have certain drawbacks on light absorption activity since they have a wide band gap. In addition, the electrochemical properties are also hindered due to the fast electron-hole pair's recombination rate. So, in order to boost the optical, electrochemical properties of ZnO NPs, the transition metal-doped ZnO nanoparticles have been introduced. Mainly transition metal ions doped ZnO NPs have intrinsic donor defects, hence leading to the increase in the surface area [1-3]. Among the doping of other transition metals, doping of Mn into the ZnO host lattice can result in large injected spins and carriers which help it suitable to be applied as a magnetic semiconductor. Similarly, doping of Ag to ZnO NPs causes oxygen vacancies and alteration of ions in light scattering patterns.

In this work, we synthesized pure ZnO, Ag-doped ZnO and Mn-doped ZnO NPs by sol-gel method and their morphological, structural and optical properties were studied and compared.

## 2. MATERIALS AND METHODS

### 2.1 Experimental methods

Zinc acetate dehydrate ( $\text{Zn}(\text{CH}_3\text{COO})_2 \cdot 2\text{H}_2\text{O}$ , 99%), Silver (I) chloride (AgCl), Manganese (II) chloride ( $\text{MnCl}_2$ ), sodium hydroxide (NaOH, 99%) and ethanol were purchased from Merck India.

Pure ZnO, Ag doped ZnO and Mn doped ZnO NPs were synthesized by Sol-Gel method. Initially, 20 g of NaOH was dissolved in 80 ml double distilled water and stirred vigorously to obtain NaOH solution. For the synthesis of pure ZnO NPs, 0.02 mole of zinc acetate was mixed with 80 ml of ethanol and stirred 2 hours at 60 °C. After that, NaOH solution was added dropwise till attained pH 11.5. Large amount of white solution were formed and this slurry were continuously stirred for 18 hours. This reactant was kept undisturbed manner for one day a white gel were formed, which was filtered and washed with distilled water and dried at 100 °C in hot air oven for 12 hrs and finally calcined at 550 °C. There is a noticeable colour change from white to dark ash color.

For the synthesis of Ag doped ZnO, 0.95 mole of zinc acetate and 0.05 mole of AgCl was added to 50 ml of ethanol and stirred well for 2 hrs at 60 °C. After that,

NaOH solution was added dropwise till attained pH 11. Large amount of white solution were formed and this slurry were continuously stirred for 18 hrs. This reactant was kept undisturbed manner for one day, a white gel were formed, which was filtered and washed with distilled water and dried at 100 °C in hot air oven for 12 hrs and finally calcined at 550 °C. The same procedure was followed for the synthesis Mn-doped ZnO also. But, instead of AgCl, the same molar amount of  $\text{MnCl}_2$  was used. The Schematic of synthesis procedure is shown in Fig 1.

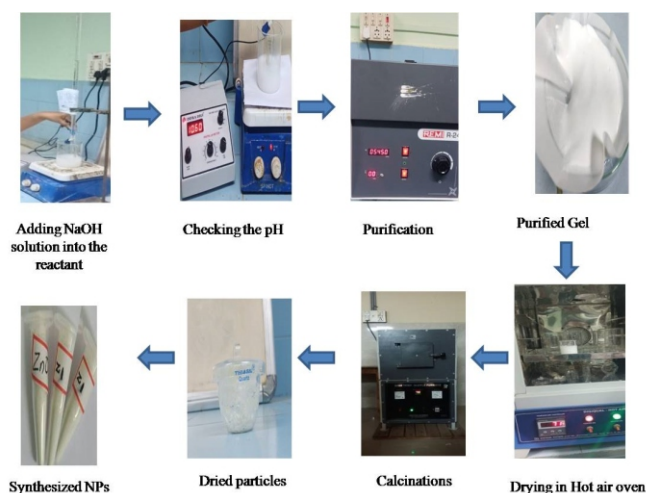


**Fig. 1** Schematic of the synthesis procedure of NPs by Sol-Gel Method

### 2.2 Characterizations of synthesized NPs

The crystalline structure and size of the synthesis NPs was examined by X-ray diffraction studies (Rigaku Ultima IV XRD spectrometer with nickel-filtered Cu-K $\alpha$  with the scan rate of 0.020), High-resolution transmission electron microscope (HR-TEM Model: JSM-7600F) analysis, Scanning electron microscope (SEM – Zeiss supra 55VP) image studies. The crystal size of the synthesized NPs were calculated by using the Scherrer formula [7-9]

$$D = (k\lambda) / (\beta \cos\theta)$$

Where D is the crystalline size, k is the Scherrer constant (0.9),  $\beta$  is the full width

half maximum (FWHM) of the diffraction peak.  $\theta$  is the Braggs angle of diffraction and  $\lambda$  is the wave length of X ray radiation.

Optical properties were examined by using UV-Vis-NIR spectrophotometer (Model: L-650 UV, Perkin Elmer) and photoluminescence (PL) spectrofluorometer (Nanolog, Horiba, Jobin Yvon). The band gap was estimated from the tauc plot (plotting  $(\alpha h\nu)^2$  Versus  $h\nu$ ) using the relation reported in elsewhere [10-13].

$$(\alpha h\nu)^2 = A_0(h\nu - E_g)$$

where  $\alpha$  represents the absorption coefficient,  $h$  is the planks constant,  $\nu$  is the frequency,  $E_g$  is the band gap and  $A_0$  is the constant which related to the effective masses associated with the bands.

### 3. RESULTS AND DISCUSSION

#### 3.1 Structural analysis

The XRD spectrum of pure ZnO, Mn-ZnO and Ag-ZnO are shown in Fig. 2. In these spectra, diffraction peaks at around  $2\theta = 31.8^\circ, 43.5^\circ, 36.39^\circ, 47.56^\circ, 56.61^\circ, 62.91^\circ$  and  $67.98^\circ$  were indexed according to (100), (002), (101), (102), (110), (103) and (112) planes of the hexagonal wurtzite crystal structures with space group P63mc (JCPDS No. 89-1397) [1, 14]. Close investigation reveals that, in XRD spectrum of Mn-doped ZnO NPs, the presence of metallic Mn diffraction peaks are not found. But, in the Ag-doped ZnO NPs, very less intense diffraction peaks of metallic Ag are observed at  $38.21^\circ$  and  $44.41^\circ$  ((111) plane and (200) plane of Ag) [15]. This may be due to the ionic radii of  $Zn^{2+}$  (0.72 Å),  $Mn^{2+}$  (0.80 Å) and  $Ag^+$  (1.22 Å) ions. That is,  $Zn^{2+}$  and  $Mn^{2+}$  has almost similar ionic size and it is lower than that of ionic size of  $Ag^+$ . Therefore, doping of Ag to ZnO crystals host causes the formation of oxygen vacancies and alteration of ions in light scattering patterns [6]. By using the Scherrer formula, the crystalline size of pure ZnO, Mn-ZnO and Ag-ZnO was calculated to be 16 nm, 22 nm and 36 nm, respectively.

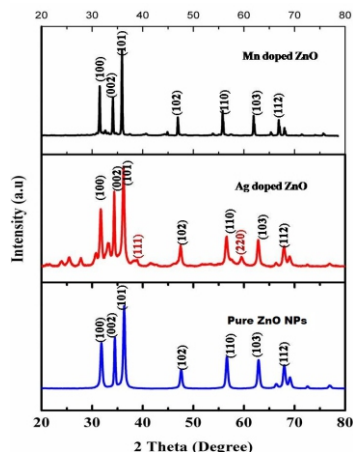


Fig. 2 XRD spectra of Pure ZnO NPs, Ag doped ZnO and MN doped ZnO

#### 3.2 Morphological analysis

The TEM image of the pure ZnO, Mn doped ZnO and Ag doped ZnO is exposed in Fig.3 (a-c) (inset: the selected area diffraction patterns). These images confirm the nano crystalline nature of the synthesized samples. From these images, the average crystal size of the pure ZnO, Mn doped ZnO and Ag doped ZnO was found to be 14 nm, 20 nm and 35 nm, respectively. This confirm the difference in the crystal size (pure ZnO < Mn doped ZnO < Ag doped ZnO).

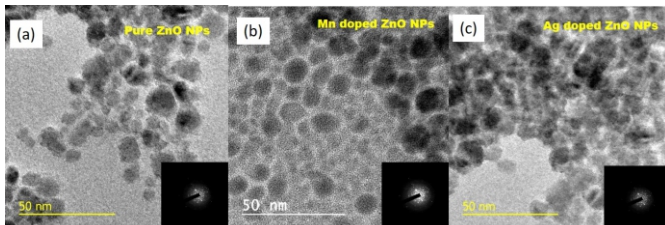


Fig. 3 TEM image and SAED pattern of (a) Pure ZnO NPs, (b) Mn doped ZnO and (c) Ag doped ZnO

The SEM image (Fig. 4 (a-c)) shows the surface nature of the synthesized NPs. From these images, it confirms that the morphology of the NPs changes while doping Mn and Ag. More than that agglomeration was very less in pure ZnO in comparison with doped ZnO. This may be due to the crystal imperfection and lattice defect, varies in lattice parameters and surface area. EDX spectra (Fig.5 (a-c)) reveals that other than Zn and O, the presence of Mn in Mn-ZnO and Ag in Ag-ZnO

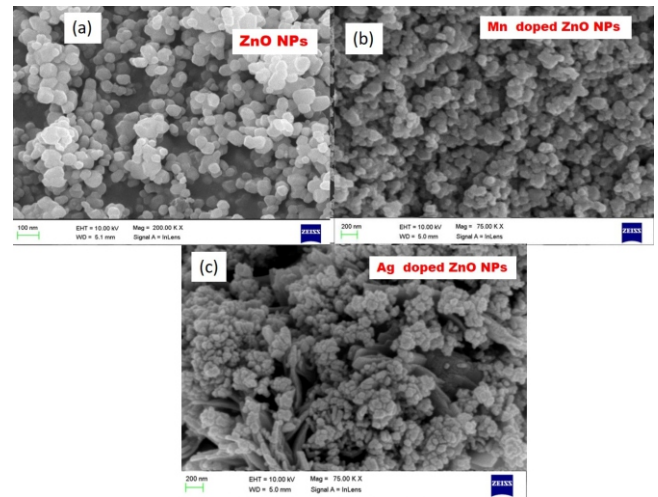


Fig. 4 SEM images of (a) Pure ZnO NPs, (b) Mn doped ZnO and (c) Ag doped ZnO

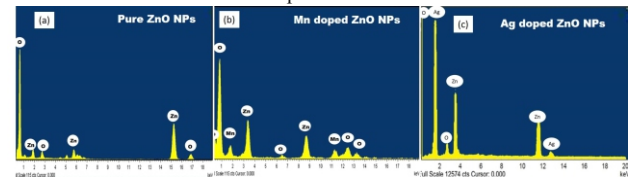


Fig. 5 EDX spectrum of (a) Pure ZnO NPs, (b) Mn doped ZnO and (c) Ag doped ZnO

#### 3.2 Optical studies

The UV-Vis absorbance spectrum of pure ZnO, Mn doped ZnO and Ag doped ZnO depicts in Fig. 6(a). These spectrum shows strong absorption maximum at around 350 to 400 nm. In the UV spectrum of the pure ZnO, the absorption peak was centered at 357 nm. This is due to the intrinsic band gap of hexagonal wurtzite structured ZnO nanocrystals. This occurs due to the transition of electron from valance band to conduction band. There is a red shift of absorption was observed while doping. This improved light absorption is due to the presence of Mn and Ag into the ZnO host [16].

The optical band gap of the pure ZnO, Mn-ZnO and Ag-ZnO was estimated from the Tauc plot (Fig.6 (b)) analysis. From this, bandgap energy is found to be 3.34 eV, 2.72 eV, and 2.51 eV for pure ZnO, Mn-ZnO and Ag-ZnO NPs, respectively. Narrowing the band gap agrees the quantum confinement effect, that is, the band gap of a semiconductor decrease while increase in the crystal size [17]. While doping Ag or Mn, the size of the NPs varies with dopant impurities. It leads to over agglomeration of impurities, results in increase in size and decrease in band gap.

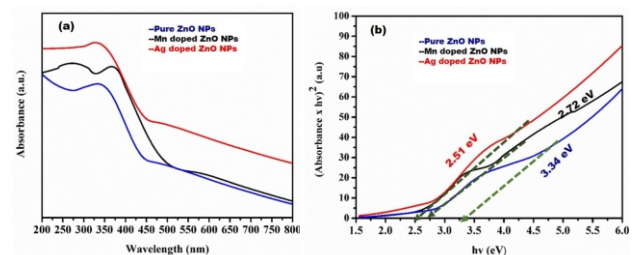


Fig. 6 (a) Uv-Vis Absorbance spectra and (b) Tauc plot Pure ZnO NPs, (b) Mn-ZnO and © Ag-ZnO

The PL emission spectra of pure ZnO, Mn-ZnO and Ag-ZnO NPs at an excitation wavelength of 325 nm is shown in Fig. 7. In all the three NPs, there is narrow emission peak was observed at 385 nm with 30 nm in peak width, indicates the free excitonic recombination in ZnO [16]. There is a decrease in intensity of the emission peaks was observed while doping in the following order: ZnO > Mn-ZnO > Ag-ZnO. Quenching in the emission intensity reveals the disrupting the recombination rate [18]. This is mainly due to the particle agglomeration [19].

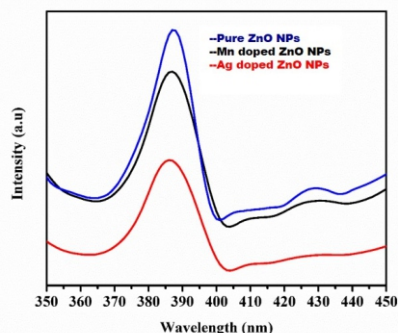


Fig. 7 PL emission spectrum of Pure ZnO NPs, Mn-ZnO and Ag-ZnO

#### 4. CONCLUSION

Pure ZnO NPs, Mn doped ZnO and Ag doped ZnO were synthesized by a sol-gel method. Its XRD spectrum analysis revealed that there is no change in the hexagonal wurtzite structures of ZnO NPs while doping with Mn or Ag. The crystalline size of pure ZnO, Mn-ZnO and Ag-ZnO was calculated to be 16 nm, 22 nm and 33 nm, respectively. SEM and TEM analysis confirms that, while doping Ag or Mn, the size of the NPs varies with respect to dopant impurities. It leads to over agglomeration of impurities, results in increase in size. Uv-vis absorption spectra reveal that Ag- ZnO NPs have broad light absorption capability compared to pure ZnO and Mn- ZnO. This is due to the narrow bandgap of Ag- ZnO NPs. Similarly, PL emission intensity of Ag doped ZnO was quenched with respect to the pure ZnO and Mn-ZnO, which exposes the disrupting the recombination rate Hence Ag-ZnO has superior optical properties.

#### Conflict of Interest

The authors declare no competing financial interest.

#### Acknowledgements

The authors gratefully acknowledge Department of Science and Technology, Wise Kiran, New Delhi for providing financial support under Women Scientist scheme A (DST/WOS-A, No. SR/WOS-A/PM-81/2018 (G) dated: 24/09/2020).

#### 5. REFERENCES

- Shamhari NM, Wee BS (2018) Synthesis and Characterization of Zinc Oxide Nanoparticles with Small Particle Size Distribution. 578–585. <https://doi.org/10.17344/acsi.2018.4213>
- Raj CJ, Joshi RK, Varma KBR (2011) Synthesis from zinc oxalate, growth mechanism and optical properties of ZnO nano / micro structures. 1188:1181–1188. <https://doi.org/10.1002/crat.201100201>
- Singh P, Kumar R, Singh RK (2019) Progress on Transition Metal-Doped ZnO Nanoparticles and Its Application. Ind Eng Chem Res 58:17130–17163. <https://doi.org/10.1021/acs.iecr.9b01561>
- Barceló I, Lana-Villarreal T, Gómez R (2011) Efficient sensitization of ZnO nanoporous films with CdSe QDs grown by Successive Ionic Layer Adsorption and Reaction (SILAR). J Photochem Photobiol A Chem 220:47–53. <https://doi.org/10.1016/j.jphotochem.2011.03.016>
- Sagadevan S, Pal K, Chowdhury ZZ, Hoque ME (2017) Structural, dielectric and optical investigation of chemically synthesized Ag-doped ZnO nanoparticles composites. J Sol-Gel Sci Technol 83:394–404. <https://doi.org/10.1007/s10971-017-4418-8>
- Ravishankar TN, Manjunatha K, Ramakrishnappa T, et al (2014) Comparison of the photocatalytic degradation of trypan blue by undoped and silver-doped zinc oxide nanoparticles. Mater Sci Semicond Process 26:7–17. <https://doi.org/10.1016/j.mssp.2014.03.027>
- Chandraprabha I, Kottayi R, Ilango V (2021) Structural and optical studies of Zinc doped TiO<sub>2</sub> nanoparticles. 13:49–55. <https://doi.org/10.9790/4861-1301024955>
- Kottayi R, Panneerselvam P, Singh N (2020) of Cu<sub>2</sub>AgInS<sub>4</sub> QDs onto porous TiO<sub>2</sub> NFs to use as an efficient photoanode to boost the photoconversion efficiency of QDSCs. New J Chem 44:13148–13156. <https://doi.org/10.1039/d0nj01699c>
- Roopakala Kottayi, Pratheep Panneerselvam, Nisha Singh, Vignesh Murugados, Ramdas Sittaramane SA\* (2020) Influence of bifunctional linker on loading of Cu<sub>2</sub>AgInS<sub>4</sub> QDs onto porous TiO<sub>2</sub> NFs to use as an effective photoanode to boost up the photoconversion efficiency of QDSC. New J Chem. <https://doi.org/10.1039/D0NJ01699C>
- Kottayi R (2021) Cu<sub>2</sub>AgInS<sub>2</sub>Se<sub>2</sub> quantum dots sensitized porous TiO<sub>2</sub> nanofibers as a photoanode for high-performance quantum dot sensitized solar cell. Int J energy Res 45:13563–13574. <https://doi.org/10.1002/er.6685>
- Kottayi R, Veerappan I, Sittaramane R (2022) Near-infrared photoactive Ag-Zn-Ga-S-Se quantum dots for high-performance quantum dot-sensitized solar cells. Beilstein J Nanotechnol 13:1337–1344. <https://doi.org/10.3762/BJNANO.13.110>
- Kottayi R, Ilango V, Sittaramane R (2022) Wide light-harvesting AgZnGaS<sub>3</sub> quantum dots as an efficient sensitizer for solar cells. Opt Mater (Amst) 134:113036. <https://doi.org/10.1016/j.optmat.2022.113036>
- Kottayi R, Ilango V, Sittaramane R (2022) Cu<sub>2</sub>AgInS<sub>4</sub> quantum dot sensitized zinc doped Titania nanoparticles film as the high efficient photoanode for photovoltaic cells. Optik (Stuttg) 255:168692. <https://doi.org/10.1016/j.jileo.2022.168692>
- Alkahlout A, Al Dahoudi N, Grobelsek I, et al (2014) Synthesis and Characterization of Aluminum Doped Zinc Oxide Nanostructures via Hydrothermal Route. J Mater 2014:1–8. <https://doi.org/10.1155/2014/235638>
- A R, M IT (2022) SYNTHESIS OF SILVER (Ag) DOPED ZINC OXIDE (ZnO) NANOPARTICLES AS EFFICIENTPHOTOCATALYTIC ACTIVITY FOR DEGRADATION METHYLENE BLUE DYE. J Adv Sci Res 13:129–135. <https://doi.org/10.55218/jasr.202213217>

- Ashebir ME, Tesfamariam GM, Nigussie GY, Gebreab TW (2018) Structural, optical, and photocatalytic activities of Ag-Doped and Mn-Doped ZnO Nanoparticles. J Nanomater 2018: <https://doi.org/10.1155/2018/9425938>
- KHAN W, KHAN ZA, SAAD AA, et al (2013) SYNTHESIS AND CHARACTERIZATION OF Al DOPED ZnO NANOPARTICLES. Int J Mod Phys Conf Ser 22:630–636. <https://doi.org/10.1142/s2010194513010775>
- Liu I, Lo H, Chien C, et al (2008) Enhancing photoluminescence quenching and photoelectric properties of CdSe quantum dots with hole accepting ligands. J Mater Chem 18:675–682. <https://doi.org/10.1039/b715253a>
- Peymannia M, Gharanjig K, Arabi AM (2020) Effect of zinc oxide quantum dots on the photovoltaic properties of natural dye-sensitized solar cells. Int J Energy Res 1–14. <https://doi.org/10.1002/er.6082>